JOURNAL OF BASIC SCIENCE AND ENGINEERING

A Hue-Based Segmentation for Melody Watermelon Images Before Harvesting

Ayesha Khannum*[1], R. Dhanesha[1], Narendra Kumar S.[2], Umesha D. K.[3], and Shrinivasa Naika C. L.[4]

[1]Department of Computer Science, Davangere University, Davangere, Karnataka, India
[1]Department of Computer Science & Engineering, J.N.N. College of Engineering, Shivamogga, Karnataka, India
[3]Department of Computer Science & Engineering, Government Polytechnic Soraba, Shivamogga, Karnataka, India
[4]Department of Computer Science & Engineering, U. B. D. T. College of Engineering, Davangere, Karnataka, India

DOI: https://doie.org/10.10399/JBSE.2026243962

Abstract

Melody watermelon, a hybrid variety valued for its uniform morphology and sweet flesh, has gained increasing importance in precision agriculture. Accurate fruit segmen-tation from on-field images is a fundamental prerequisite for downstream tasks such as yield estimation, maturity assessment, and sweetness identification. However, existing segmentation approaches, particularly deep learning and clustering-based methods, are often computationally intensive and less robust under complex field conditions. The study proposes a lightweight, hue-based segmentation framework using the HSV color model to isolate Melody watermelons from natural field backgrounds. The method retains pixels with hue values above a selected threshold and applies multi-stage fil-tering, including Gaussian, median, and averaging filters, followed by morphological refinement to enhance boundary delineation and suppress background noise such as soil and foliage. An ablation study is conducted to analyze the impact of different hue thresholds, leading to the selection of an optimal configuration. Segmentation perfor-mance is evaluated against ground truth annotations using standard metrics, including Dice Similarity Coefficient, Intersection over Union, Precision, Recall, F1-score, and Volumetric Overlap Error, achieving a Dice coefficient of up to 0.96. A comparative analysis further confirms the robustness and effectiveness of the proposed approach for real-field agricultural applications.

Keywords: HSV color space, Hue-based segmentation, Binary mask, Gaussian filtering, Median filtering (medfilt3), Morphological erosion, Hole filling.

1 Introduction

Watermelon (Citrullus lanatus) is a globally important horticultural crop, where accurate harvest-time estimation directly affects fruit quality, sweetness, and market value. Melody watermelon, a widely cultivated hybrid variety, requires reliable pre-harvest monitoring to ensure optimal yield. Traditional sweetness assessment methods depend heavily on manual inspection and farmer experience, which are labor-intensive, subjective, and difficult to scale under large-field cultivation.

With the advancement of precision agriculture, image-based techniques have become es-sential for automated crop monitoring. Among these, accurate segmentation of fruits from complex field backgrounds is a critical prerequisite for applications such as size estimation, maturity analysis, yield prediction, and automated harvesting. The study deliberately fo-cuses exclusively on fruit segmentation, recognizing it as a foundational step for downstream sweetness and quality assessment. However, reliable segmentation in real-field environments remains challenging due to uncontrolled illumination, occlusions caused by foliage, soil in-terference, and variability in fruit appearance.

Deep learning-based segmentation models, including U-Net and YOLO variants, have demonstrated high accuracy in controlled settings. Nevertheless, these approaches often re-quire large labeled datasets, extensive training, and high computational resources, which limit their practical deployment in resource-constrained agricultural environments. In addi-tion, their black-box nature raises concerns regarding interpretability and robustness when applied under varying field conditions.

In contrast, classical image processing methods offer advantages in terms of computa-tional efficiency, transparency, and ease of deployment. Color-based segmentation using the HSV color space, particularly the Hue component, is well suited for outdoor agricultural imaging due to its reduced sensitivity to illumination variations. Despite this potential, many existing classical approaches rely on heuristic parameter selection, are evaluated on limited datasets, and lack systematic validation through ablation and comparative analysis, restricting their reliability for real-field deployment.

To address these limitations, the study proposes a training-free, hue-based segmentation framework for isolating Melody watermelons from complex field environments. The method combines Hue thresholding with multi-stage filtering and morphological refinement to achieve accurate fruit segmentation without requiring high performance hardware or model train-ing. The framework is evaluated on manually annotated real-field images and is supported by a systematic ablation study and a comparative analysis against an existing segmenta-tion approach. Experimental results demonstrate that the proposed lightweight framework achieves performance comparable to more computationally intensive techniques, highlighting its suitability for practical precision agriculture applications.

The main contributions of this work are summarized as follows:

- A training-free and explainable hue-based segmentation framework for accurate isola-tion of Melody watermelons under real-field conditions.
- A large-scale real-field evaluation using manually annotated images, enabling statisti-cally reliable performance assessment.

- A systematic ablation study analyzing the sensitivity of hue threshold selection, which is rarely reported for classical segmentation approaches.
- A comparative analysis demonstrates competitive performance against an existing seg-mentation method while maintaining low computational complexity.
- A deployment-oriented design emphasizes efficiency, robustness, and suitability for resource-constrained agricultural environments.

To quantitatively assess the effectiveness of the proposed segmentation framework, the following subsection describes the overlap- and region-based performance metrics used to evaluate the agreement between the segmented outputs and the corresponding ground truth masks.

1.1 Segmentation Performance Metrics

The effectiveness of the proposed segmentation framework is quantitatively evaluated using widely adopted performance metrics, including Dice Similarity Coefficient (DSC) [1], Intersection over Union (IoU) [2], Precision, Recall, F1-score [3], and Volumetric Overlap Error (VOE) [4]. These metrics measure the spatial agreement between the predicted segmentation masks and the corresponding ground truth annotations at the pixel level.

Let A denote the ground truth mask and B the predicted segmentation mask. The Dice Score, defined in Equation 1, measures the degree of overlap between A and B [1]. Intersection over Union (IoU), also known as the Jaccard Index, is given in Equation 2 and quantifies the ratio of the intersection to the union of the two masks [2].

$$\text{Dice Score} = \frac{2 \times |Aa \cap Bb|}{|Aa| + |Bb| + \epsilon} \tag{1}$$

$$\text{IoU (Jaccard Index)} = \frac{|Aa \cap Bb|}{|Aa \cup Bb| + \epsilon} \tag{2}$$

Precision and Recall, defined in Equations 3 and 4, evaluate the accuracy of foreground prediction by measuring false positives and false negatives, respectively [3]. The F1-score, shown in Equation 5, represents the harmonic mean of Precision and Recall, providing a balanced assessment of segmentation performance.

$$\text{Precision} = \frac{P\,t}{P\,t + P\,f + \epsilon} \tag{3}$$

$$\text{Recall} = \frac{P\,t}{P\,t + N\,f + \epsilon} \tag{4}$$

$$\text{F1-Score} = \frac{2 \times (\text{Precision} \times \text{Recall})}{\text{Precision} + \text{Recall} + \epsilon} \tag{5}$$

The Volumetric Overlap Error (VOE), defined in Equation 6, quantifies the dissimilarity between the predicted and ground truth masks [4]. Lower VOE values indicate better segmentation accuracy.

$$VOE = 1 - \frac{|Aa \cap Bb|}{|Aa \cup Bb|} \times 100\% \quad (6)$$

where:

- P t denotes true positives, representing correctly segmented foreground pixels;
- P f denotes false positives, where background pixels are incorrectly classified as fore-ground;
- N f denotes false negatives, where foreground pixels are incorrectly classified as back-ground;
- ϵ is a small constant added to avoid division by zero.

These metrics collectively provide a comprehensive and objective assessment of segmen-tation accuracy, overlap quality, and error characteristics, enabling reliable comparison with existing state-of-the-art methods. The following section surveys existing literature on fruit segmentation and related image processing techniques to position the proposed method within the current state of research.

2 Related Work

Several studies have explored classical image processing techniques for fruit segmentation using color information and morphological operations. R. Dhanesha and C. L. S. Naika [5] segmented arecanut fruits using the HSV color model combined with thresholding and mor-phological operations, achieving accuracy in the range of 85–90% and evaluating performance using VOE and DSC. In a subsequent work, the same authors [6] employed active contour models for arecanut segmentation, reporting VOE values ranging from –0.0010 to –0.2852 and DSC values between 0.0075 and 0.0028. R. Dhanesha et al. [7] further investigated the YCgCr color model for arecanut segmentation, achieving an accuracy of 80%. These studies demonstrate the applicability of classical color-based and contour-based methods, although their performance is often dependent on heuristic parameter selection and limited validation.

For fruit detection and yield estimation, G. K. Wuzor and N. C. Woods [8] proposed a method combining k-means clustering, watershed segmentation, morphological operations, and connected component labeling for guava detection, achieving 94.5% precision, 84.4% recall, and a counting accuracy of 92.4%. These approaches highlight the effectiveness of classical segmentation pipelines for fruit localization, while also indicating sensitivity to background complexity and illumination conditions.

In addition to segmentation, several studies have focused on fruit ripeness and sweetness classification using acoustic, image-based, and hybrid features. Pavadharini T. et al. [9] classified watermelons using acoustic features with Naive Bayes, SMO, and Random Tree classifiers, achieving an accuracy of 78.8%. K. Chawgien and S. Kiattisin [10] improved watermelon sweetness detection by fusing sound and image features with multiple machine learning models, reporting a maximum accuracy of 92% using Gradient Boosted Trees. R.

Dhanesha et al. [11] proposed a hybrid segmentation and classification framework for are-canut using HSV, YCbCr, and YPbPr color spaces with a Random Forest classifier, achieving segmentation performance evaluated through VOE and DSC and a classification accuracy of 87.81%.

With the advancement of deep learning, convolutional neural network–based segmenta-tion approaches have been widely adopted in agricultural applications. C. Qian et al. [12] improved the U-Net architecture by incorporating VGG16 and Residual Channel Attention (RCCA) for melon segmentation, achieving a mean pixel accuracy of 98.83% and a mean IoU of 96.67%. Another study [13] proposed a crop seedling segmentation framework using an edge information fusion model and compared it with the traditional U-Net architecture across RGB, grayscale, and color image datasets. The results demonstrated improvements in pixel accuracy, mean IoU, precision, and F1-score through the integration of semantic and edge features.

Deep learning has also been applied extensively for watermelon classification and detec-tion. M. Fitria et al. [15] investigated CNN-based models such as EfficientNet, ResNet, and ShuffleNet for watermelon sweetness classification, reporting an accuracy of 92.22% us-ing EfficientNet-B7. For robotic detection, Y. Rong et al. [14] enhanced YOLOv5s with a Convolutional Block Attention Module (CBAM), achieving a precision of 89.8%, represent-ing a 2.4% improvement over baseline models. A. C. Anitha et al. [16] integrated U-Net^2 and YOLOv4 for arecanut segmentation and yield estimation, achieving training and val-idation accuracies of 88% and 85%, respectively. L. Jiang et al. [17] employed YOLOv8s with panoramic image stitching for watermelon detection and yield estimation, achieving a counting accuracy of 97.2%.

Other studies have explored multimodal and real-time systems for ripeness detection. Y. W. Lin et al. [18] developed an AI- and IoT-based system using acoustic analysis for watermelon ripeness detection, achieving an accuracy of 94.07%. A lightweight DFU (Double-depth Convolution and Fusion block U-Net) model was proposed in [19] for crop plant detection under real-field conditions, reporting F1-score values above 92% for multiple crops. Z. M. Choffin et al. [20] utilized microwave imaging with DAS beamforming and CNNs for ripeness detection, achieving an accuracy of 86%.

Overall, studies published between 2018 and 2025 demonstrate significant progress in fruit segmentation and classification, with a clear shift from classical image processing techniques to deep learning–based approaches employing U-Net variants, YOLO architectures, and attention mechanisms. While recent methods often report high numerical accuracy, they typically rely on large annotated datasets, extensive training, and substantial computational resources. Moreover, many works lack systematic parameter sensitivity analysis, ablation studies, and deployment-oriented evaluation under real-field conditions.

Building upon these observations, the present study focuses on developing an efficient and explainable segmentation framework that emphasizes real-field applicability, systematic ablation analysis, and comparative validation, thereby addressing key limitations observed in existing literature. The following section presents the proposed segmentation methodology in detail.

3 Methodology

3.1 Dataset Preparation

The dataset used in the study consists of on-field images of Melody watermelon collected from agricultural fields in Kakkol village, Kadaramundagi, Byadgi, Haveri district, Karnataka, India. Images were captured under natural outdoor conditions, incorporating realistic vari-ations in illumination, background clutter, and occlusions caused by soil, leaves, and vines. Data acquisition was performed across multiple field visits during the crop growth period to ensure diversity in visual appearance. Representative samples from the data collection process are shown in Figure 1.

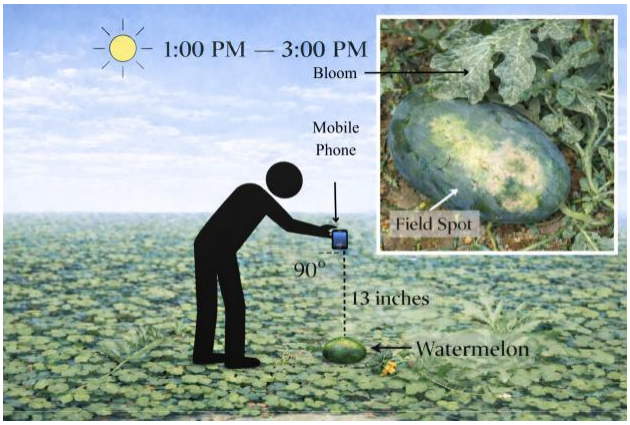

Figure 1: Representative Melody watermelon images acquired under real-field cultivation conditions.

All images were captured using a handheld camera at a fixed distance of approximately 13 inches and a viewing angle of 90°, ensuring consistency in scale and perspective. The dataset was collected from a 2.5-acre agricultural field with the assistance of local farmers. All images were stored in JPEG format and resized to a uniform resolution of 512 × 512 pixels prior to processing.

Pixel-level ground truth segmentation masks were manually annotated using the Inkscape tool to accurately delineate watermelon regions from the background. These annotations were used as reference data for quantitative evaluation of the segmentation performance. Although images were acquired at different maturity stages, the present study focuses exclu-sively on watermelon fruit segmentation, and all images are treated as a single segmentation class. The complete dataset is publicly available at the repository [21]. Based on this anno-tated dataset, the following section details the proposed hue-based segmentation methodol-ogy employed to accurately isolate watermelon regions from complex field backgrounds.

3.2 Segmentation Methodology

The proposed segmentation framework is designed to accurately isolate watermelon re-gions from complex field backgrounds using a lightweight and explainable image processing pipeline. All input images were loaded in JPEG format and resized to a uniform resolution

(a) (b) (c)

Figure 2: Sample images of Melody watermelons captured at different time periods during the cultivation cycle.

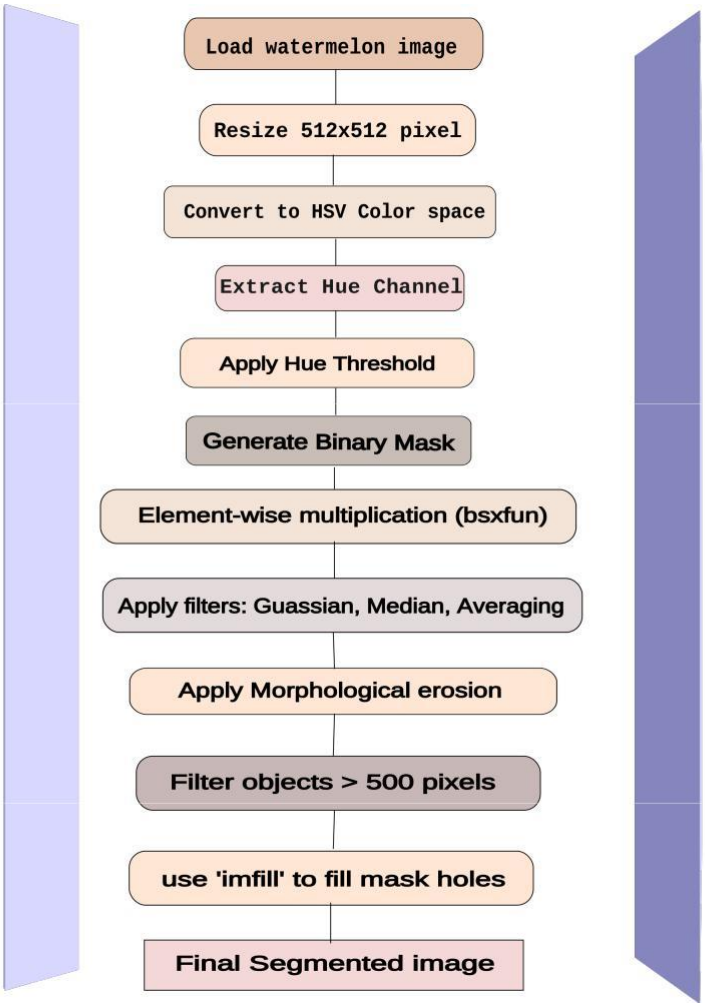

Figure 3: Segmentation pipeline for Melody Watermelon Segmentation

Vol. 23, No. 1, (2026)
ISSN: 1005-0930

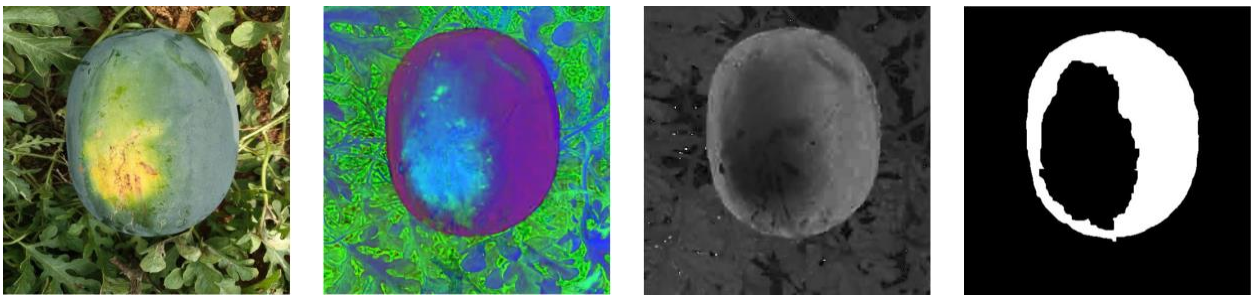

(a) Original image (b) HSV image (c) Hue channel (d) Binary mask

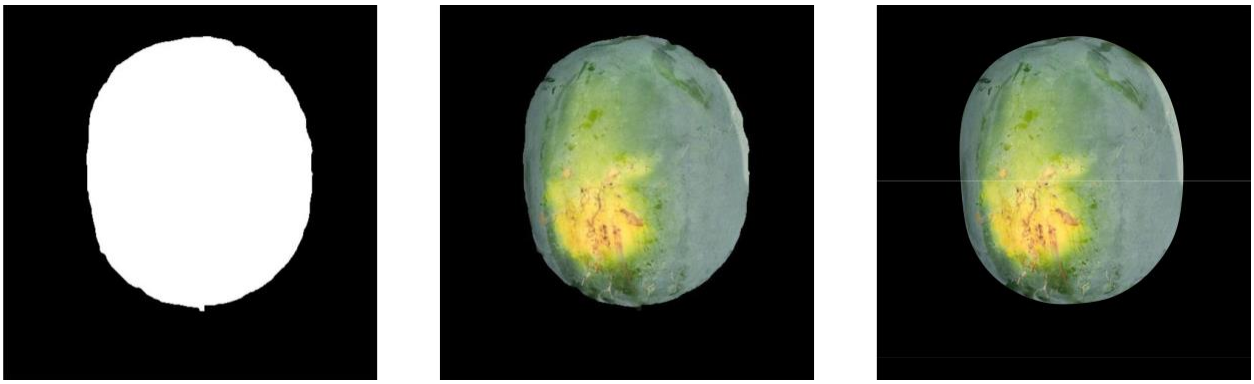

(e) Hole-filled mask (f) Final segmented image (g) Ground truth

Figure 4: Step-by-step illustration of the proposed hue-based segmentation process for Melody watermelon images.

of 512 × 512 pixels to ensure consistency during processing. The images were then converted from the RGB color space to the HSV (Hue Saturation Value) color model, which effectively separates chromatic information from illumination and is well suited for outdoor agricultural environments. Among the HSV components, the Hue channel was extracted, as it directly represents color information and is less sensitive to lighting variations. Figure 4 illustrates the complete step-by-step segmentation workflow, starting from the original input image (Figure 4a) and its conversion to the HSV color space (Figure 4b). From the HSV representation, the Hue channel was isolated (Figure 4c), as it provides effective chromatic discrimination between the watermelon surface and background elements.

A fixed hue threshold of 0.3 was applied to the extracted Hue channel to generate an initial binary mask (Figure 4d), where pixels corresponding to watermelon regions were retained while background components such as soil and foliage were suppressed. This threshold was empirically selected, and its effectiveness is further validated through a systematic ablation study presented in a later section.

The resulting binary mask was cast to the same data type as the original image to ensure pixel-wise compatibility and applied using element-wise multiplication, preserving only the relevant fruit regions. To reduce noise and improve boundary smoothness, a multi-

stage filtering strategy was employed. Gaussian filtering with a standard deviation ofσ = 2 was first applied to suppress high-frequency noise, followed by median filtering using a 3× 3 × 3 neighborhood to eliminate impulse noise while preserving edges. An averaging filter with a 5 × 5 kernel was subsequently applied to enhance regional homogeneity and stabilize the segmentation output.

Morphological refinement was then performed to further improve segmentation quality. Erosion was applied three times using a disk-shaped structuring element with a radius of 3 to remove thin artifacts and weak connections. Small connected components with an area smaller than 500 pixels were removed to eliminate spurious regions. The refined binary mask was then subjected to hole filling (Figure 4e) to ensure that the segmented watermelon regions were continuous and complete.

Finally, the refined mask was applied to the original image using element-wise multipli-cation to obtain the final segmented output (Figure 4f). The accuracy of the segmentation results was visually validated by comparison with the corresponding manually annotated ground truth mask (Figure 4g), demonstrating close alignment between the predicted wa-termelon boundaries and the reference annotations. The sensitivity of the proposed seg-mentation framework to the hue threshold parameter is systematically evaluated through an ablation study in the following section.

3.3 Ablation Study

An ablation study was conducted to systematically analyze the influence of the hue threshold parameter on the segmentation performance of the proposed framework. Since the Hue channel plays a central role in separating watermelon regions from complex field backgrounds, different threshold values were evaluated to identify a suitable operating point. Specifically, hue thresholds greater than that of 0.20, 0.25, 0.30, 0.35, and 0.40 were examined while keeping all other preprocessing, filtering, and morphological operations unchanged.

Quantitative evaluation was performed on the complete image dataset using standard segmentation metrics, including Dice Similarity Coefficient (DSC), Intersection over Union (IoU), Precision, Recall, and Volumetric Overlap Error (VOE). The mean performance values obtained for each threshold configuration are summarized in Table 1.

Table 1: Ablation study evaluating the impact of different hue threshold values on segmentation performance

Hue Threshold	Dice	IoU	Precision	Recall	F1-Score	VOE
> 0.20	0.7081	0.5698	0.5759	0.9747	0.7081	0.4302
> 0.25	0.8999	0.8301	0.8462	0.9759	0.8999	0.1699
> 0.30	0.9609	0.9307	0.9709	0.9573	0.9609	0.0693
> 0.35	0.9206	0.8738	0.9797	0.8906	0.9206	0.1262
> 0.40	0.8286	0.7484	0.9763	0.7628	0.8286	0.2516

Figure 5a illustrates the segmentation results obtained using a hue threshold greater than 0.20. While this lower threshold successfully captures most watermelon regions, it also introduces significant background interference from soil and surrounding vegetation, leading to increased false positives and reduced precision.

The segmentation outputs corresponding to a hue threshold greater than 0.25 are shown in Figure 5b. Compared to the 0.20 threshold, background suppression is moderately im-

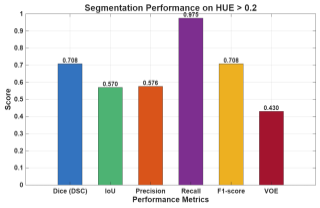

(a) Hue > 0.20

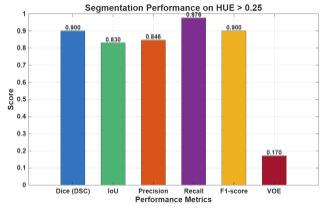

(b) Hue > 0.25

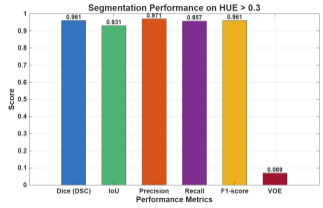

(c) Hue > 0.30

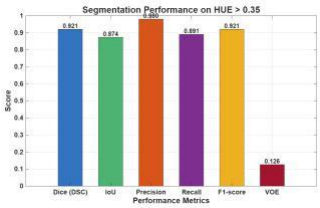

(d) Hue > 0.35

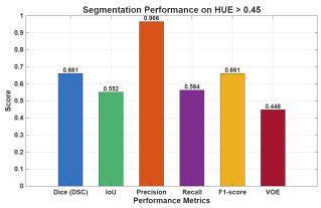

(e) Hue > 0.40

Figure 5: Qualitative segmentation results for different hue threshold conditions (Hue > T).

proved; however, residual non-fruit regions remain visible, indicating that the threshold is still insufficiently restrictive under complex field conditions.

Figure 5c presents the segmentation results obtained with a hue threshold greater than 0.30. This configuration demonstrates a clear improvement in boundary delineation and background suppression, producing segmentation masks that closely align with the ground truth annotations. The improved visual quality is further supported by the highest Dice and IoU values reported in Table 1, indicating an optimal balance between precision and recall.

As shown in Figure 5d, increasing the hue threshold greater than 0.35 results in partial loss of watermelon regions, particularly along object boundaries. Although background noise is further reduced, the segmentation becomes overly conservative, leading to increased false negatives and reduced recall.

Figure 5e illustrates the segmentation results for a hue threshold greater than that of 0.40. At this threshold level, substantial portions of the watermelon surface are excluded from the segmented regions, resulting in fragmented outputs and a noticeable decline in overlap with the ground truth masks.

Overall, the ablation study demonstrates that lower hue thresholds tend to over-segment background regions, whereas higher thresholds lead to under-segmentation of the fruit. Among the evaluated configurations, a hue threshold greater than that of 0.30 consistently achieves the most favorable trade-off between background suppression and fruit region preser-vation. Consequently, this threshold value is selected for all subsequent experiments, includ-ing comparative analysis and final performance evaluation. Using the optimal hue threshold identified above, the segmentation performance of the proposed method is evaluated in the next section.

Vol. 23, No. 1, (2026)
ISSN: 1005-0930

3.4 Segmentation Performance Evaluation

Following the ablation study, the segmentation performance of the proposed framework was evaluated using the optimal configuration identified therein. Based on the analysis of varying hue thresholds, a hue value greater than that of 0.30 was selected and fixed for all subsequent evaluations. The performance of the final segmentation pipeline was assessed using standard quantitative metrics, including Dice Similarity Coefficient (DSC), Intersection over Union (IoU), Precision, Recall, F1-Score, and Volumetric Overlap Error (VOE).

The overall segmentation results indicate a high degree of spatial agreement between the predicted segmentation masks and the corresponding ground truth annotations. The Dice and IoU metrics demonstrate strong overlap between segmented regions and reference masks, confirming accurate delineation of watermelon boundaries under real-field conditions. The achieved precision and recall values further indicate that the proposed method effec-tively suppresses background regions while preserving the complete fruit area, resulting in a balanced segmentation outcome.

The close correspondence between Precision and Recall reflects the stability of the seg-mentation process, with minimal bias toward either over-segmentation or under-segmentation. The F1-Score, serving as a harmonic measure of these two metrics, reinforces the consistency of the final segmentation results. In addition, the low VOE values observed confirm minimal disagreement between the predicted and ground truth regions, indicating precise boundary extraction.

Overall, the quantitative evaluation demonstrates that the proposed hue-based segmentation framework provides accurate and reliable segmentation without the need for training data or complex model optimization. The robustness of the final configuration highlights the effectiveness of classical color-based segmentation when combined with appropriate filtering and morphological refinement. These results establish a strong foundation for further comparative analysis against existing segmentation approaches and for deployment in practical precision agriculture applications. Building on these results, a comparative analysis with existing segmentation approaches is presented in the next section to further assess the robustness and effectiveness of the proposed framework.

3.5 Comparative Study

To further validate the effectiveness of the proposed hue-based segmentation framework, a comparative study was conducted against an existing segmentation approach reported in the literature, namely the FruitSeg30 method [22]. The comparison was performed using identical evaluation metrics to ensure fairness and consistency. These metrics include Pre-cision, Recall, F1-Score, Intersection over Union (IoU), Dice Similarity Coefficient (DSC), and Volumetric Overlap Error (VOE).

Table 2 presents a quantitative comparison between the proposed method and the Fruit-Seg30 approach [22]. As observed, the FruitSeg30 method exhibits low Precision and Recall values, resulting in weak overlap-based metrics such as IoU and Dice. The high VOE reported for FruitSeg30 indicates substantial disagreement between the predicted segmentation masks and the corresponding ground truth annotations, reflecting limited segmentation accuracy under the evaluated conditions.

Table 2: Comparison of segmentation performance between the proposed method and the FruitSeg30 approach

Metric	Proposed Method	FruitSeg30 [22]
Precision	0.9709	0.0906
Recall	0.9573	0.2374
F1-Score	0.9609	0.1129
Intersection over Union (IoU)	0.9307	0.0673
Dice Similarity Coefficient (DSC)	0.9609	0.1129
Volumetric Overlap Error (VOE)	0.0693	0.9327

In contrast to the FruitSeg30 method [22], the proposed framework achieves consistently high scores across all evaluation metrics, indicating strong spatial alignment between predicted segmentation masks and ground truth annotations. The balanced Precision and Recall values demonstrate the method's ability to accurately isolate watermelon regions while effec-tively suppressing background elements. The corresponding high F1-Score and Dice values further confirm the robustness and consistency of the segmentation results.

The performance gap between the two approaches can be attributed to the design philosophy of the proposed method. By leveraging hue-based color discrimination combined with multi-stage filtering and morphological refinement, the proposed framework effectively handles complex field backgrounds without reliance on learning-based models or extensive training data. In contrast, the comparative method [22] exhibits sensitivity to background variability, leading to under-segmentation and fragmented outputs.

Overall, the comparative analysis highlights the superiority of the proposed segmenta-tion framework in terms of accuracy, robustness, and reliability. These results reinforce the suitability of the proposed method for real-field agricultural applications, particularly in scenarios where computational efficiency, explainability, and consistent performance are essential. The following section concludes the study by summarizing the key findings and outlining potential directions for future work.

4 Conclusion

The study presented a robust and computationally efficient segmentation framework for iso-lating Melody watermelons from complex field backgrounds using classical image processing techniques. By leveraging hue information from the HSV color space in combination with multi-stage filtering and morphological refinement, the proposed method achieved accurate and reliable fruit segmentation under real-field conditions without reliance on training data or deep learning models.

The effectiveness of the framework was systematically validated through an ablation study, which identified an optimal hue threshold that balances background suppression and preservation of the fruit region. Quantitative evaluation using standard segmentation metrics, including Dice Similarity Coefficient, Intersection over Union, Precision, Recall, F1-Score, and Volumetric Overlap Error, demonstrated strong spatial agreement between the segmented outputs and ground truth annotations. The low overlap error and high con-

sistency across metrics confirm the robustness of the proposed approach. A comparative analysis against an existing segmentation method further highlighted the superiority of the proposed framework in terms of accuracy and reliability. The results indicate that the pro-posed hue-based strategy effectively handles challenging field conditions such as background clutter and illumination variations, while maintaining low computational complexity and high explainability. These characteristics make the method particularly suitable for deploy-ment in precision agriculture scenarios where efficiency and interpretability are essential.

Overall, this work establishes a strong foundation for automated fruit analysis by demon-strating that carefully designed classical segmentation techniques can rival more complex ap-proaches in real-world agricultural environments. Future work will focus on extending this segmentation pipeline toward integrated decision-support systems, including fruit classifica-tion and quality assessment based on color, texture, and shape attributes. Additionally, the development of lightweight, farmer-oriented software tools and edge-device implementations will be explored to facilitate large-scale adoption and practical deployment in smart farming applications.

References

[1] L. R. Dice, “Measures of the amount of ecologic association between species,” Ecology, vol. 26, no. 3, pp. 297–302, Jul. 1945.
[2] P. Jaccard, “The distribution of the flora in the alpine zone,” New Phytologist, vol. 11, no. 2, pp. 37–50, Feb. 1912.
[3] D. M. W. Powers, “Evaluation: From precision, recall and F-measure to ROC, informed-ness, markedness and correlation,” Journal of Machine Learning Technologies, vol. 2, no. 1, pp. 37–63, 2011.
[4] A. A. Taha and A. Hanbury, “Metrics for evaluating 3D medical image segmenta-tion: Analysis, selection, and tool,” BMC Medical Imaging, vol. 15, no. 29, pp. 1–28, Jun. 2015.
[5] Dhanesha, R., & Shrinivasa, N. C. (2018, December). Segmentation of arecanut bunches using HSV color model. In 2018 International Conference on Electrical, Electronics, Communication, Computer, and Optimization Techniques (ICEECCOT) (pp. 37-41). IEEE.10
[6] Dhanesha, R., & Shrinivasa Naika, C. L. (2018). A Novel Approach for Segmentation of Arecanut Bunches Using Active Contouring. In Integrated Intelligent Computing, Communication and Security (pp. 677-682). Singapore: Springer Singapore.
[7] Dhanesha, R., Naika, C. S., & Kantharaj, Y. (2019, July). Segmentation of arecanut bunches using YCgCr color model. In 2019 1st International Conference on Advances in Information Technology (ICAIT) (pp. 50-53). IEEE.
[8] Wuzor, G. K., & Woods, N. C. (2020). On tree guava fruit detection and yield estima-tion. Int. J. Sci. Engg. Res, 11(5), 723-731.
[9] Pavadharini, T., & Anita, H. B. (2020). Classification of Watermelon using Sound Pro-cessing. International Journal of Engineering and Advanced Technology, 9, 2489-2492.
[10] Chawgien, K., & Kiattisin, S. (2021). Machine learning techniques for classifying the sweetness of watermelon using acoustic signal and image processing. Computers and Electronics in Agriculture, 181, 105938.
[11] Dhanesha, R., Umesha, D. K., Naika, C. S., & Girish, G. N. (2021, October). Segmenta-tion of Arecanut bunches: A comparative study of different color models. In 2021 IEEE Mysore Sub Section International Conference (MysuruCon) (pp. 752-758). IEEE.
[12] Qian, C., Liu, H., Du, T., Sun, S., Liu, W., & Zhang, R. (2022). An improved U-Net network-based quantitative analysis of melon fruit phenotypic characteristics. Journal of Food Measurement and Characterization, 16(5), 4198-4207.

[13] X. Zuo, H. Lin, D. Wang and Z. Cui, ”A Method of Crop Seedling Plant Segmentation on Edge Information Fusion Model,” in IEEE Access, vol. 10, pp. 95281-95293, 2022, doi: 10.1109/ACCESS.2022.3187825.

[14] Rong, J., Fu, J., Zhang, Z., Yin, J., Tan, Y., Yuan, T., & Wang, P. (2022). Development and Evaluation of a Watermelon-Harvesting Robot Prototype: Vision System and End-Effector. Agronomy, 12(11), 2836. https://doi.org/10.3390/agronomy12112836

[15] Fitria, M., Al-Assad, M. H., Candra, Y., Roza, S., & Dawood, R. (2023, December). Pre-liminary results of a deep learning model for classifying watermelon sweetness through field-spot detection. In 1st International Conference on Business and Technological Ad-vancement in Industrial Revolution 4.0 (p. 43).

[16] Chikkalingaiah, A. A., Dhanesha, R., Palya, S. N. C., Laxmana, K. A. N., Puttaswamy, A. M., & Ayengar, P. (2024) Segmentation and yield count of an arecanut bunch using deep learning techniques. Int J Artif Intell ISSN, 2252(8938), 543.

[17] Jiang, L., Jiang, H., Jing, X., Dang, H., Li, R., Chen, J.,& Fu, L. (2024). UAV-based field watermelon detection and counting using YOLOv8s with image panorama stitching and overlap partitioning. Artificial Intelligence in Agriculture, 13, 117-127.

[18] Lin, Yun-Wei, et al. ”Watermelons Talk: Predicting Ripeness through Tapping.” IEEE Internet of Things Magazine 7.4 (2024): 154-161.

[19] H. Shi, D. Shi, S. Wang, W. Li, H. Wen and H. Deng, “Crop plant automatic de-tecting based on in-field images by lightweight DFU-Net model,” J. of Computers and Electronics in Agriculture, vol. 217, p. 108649, 2024.

[20] Choffin, Z. M., Kong, L., Gan, Y., & Jeong, N. (2025). A CNN-Based Microwave Imagining System for Detecting Watermelon Ripeness. IEEE Access.

[21] AyeshaKhannum05. (2025). Ripeness-Project:dataset. GitHub. Retrieved July 17, 2025, from https://github.com/AyeshaKhannum05/Ripeness-Project/tree/main/Augmented

[22] [22] F. M. J. M. Shamrat, R. Shakib, M. Y. I. Idris, B. Akter, and X. Zhou, “Fruit-Seg30 Segmentation dataset & mask annotations: A novel dataset for diverse fruit segmentation and classification,” Data in Brief, Elsevier, vol. 56, p. 110821, 2024, doi: 10.1016/j.dib.2024.110821.